

# The Impact of the Lightning Surge on SiC-based Medium-voltage Three-phase Four-wire Grid-connected Converters

Haiguo Li<sup>1\*</sup>, Yiwei Ma<sup>1</sup>, Shiqi Ji<sup>1</sup>, Fred Wang<sup>1,2</sup>

<sup>1</sup>Min H. Kao Department of Electrical Engineering and Computer Science, the University of Tennessee, Knoxville, TN, USA

<sup>2</sup>Oak Ridge National Laboratory, Oak Ridge, TN, USA

\*hli96@vols.utk.edu

**Abstract**—The surge voltage induced by lightning will generate an inrush current in a grid-connected converter. It may not be large in Si-based converters because of the large grid side inductive filter. However, for SiC-based multi-level converters, the inrush current could be very large due to the small filter inductance, which is selected based on the current harmonic consideration. Most previous work focuses on system-level lightning protection while the converter-level impact, especially the internal components of the converter, is rarely discussed. This paper presents the analysis of the impact of the lightning surge on a 10 kV SiC MOSFET-based 13.8 kV three-phase four-wire grid-connected converter. The IEEE arrester model and the combined wave generator model in IEC 61000-4-5 standard are used to evaluate the inrush current, DC-link overvoltage, and component-to-ground potential of the converter. Analysis and simulation results have been provided to demonstrate the impact of lightning on the grid-connected converter. It is found that large inrush current occurs due to the small filter inductance, and the neutral-to-ground impedance impacts both the inrush current and the neutral point-to-ground potential.

**Keywords**—Lightning surge, inrush current, grid-connected converter, arrester model, combined wave generator model

## I. INTRODUCTION

As one of the grid transients, the lightning surge could affect grid-connected converters. Although arresters are used at the grid side of the converter, the overvoltage induced by the lightning surge and then clamped by the arrester is still much higher than the normal grid voltage. As a result, inrush current and DC-link overvoltage could occur in the grid-connected converters during a lightning surge. If it is not considered in the converter design, it may trigger the converter protection or even damage components.

In Si-based converters, the grid-side filter inductor is relatively large, and it can help to prevent the converter from a large inrush current during the lightning surge. The 60 Hz transformer, if used, will also contribute to the reduction of the inrush current because of its inductive impedance. Also, any other impedance in the loop, such as line impedance, that the lightning surge current flowing through, will help to reduce the inrush current to the converter. For three-phase three-wire converter, the phase-to-ground impedance could be large, which will also help to avoid a large inrush current. However, for SiC-based multilevel grid-connected three-phase four-wire converters, the grid side filter inductor is small [1], if it is selected based on the grid-side current harmonic consideration. Therefore, the impact of the lightning surge on the converter operation has to be understood and taken into consideration in the converter design.

System-level protection from the lightning surge in the wind turbine, solar, and HVDC converter station has been discussed in [2]-[7]. In [2]-[3], a lightning surge current is directly imposed on the HVDC-based wind farm and turbine blade respectively, and the voltage stresses occurring inside the system and turbine are investigated with EMTP. In [4]-[5], high surge currents, emulating the lightning surge, are injected into the solar photovoltaic system on the PSCAD/EMTDC platform, and the voltage surges are analyzed. The lightning overvoltage and protection of the HVDC converter station are analyzed in [6]-[7]. However, there have been few discussions about the impact of the lightning surge on converter internal components or converter design. Also, using a current source to emulate the lightning surge need a clear understanding of the overall system impedance, which may be unknown when designing a converter.

In this paper, the impact of the lightning surge on a grid-tied three-phase four-wire converter based on cascaded H-bridge (CHB) with 10 kV SiC MOSFET is discussed. Compared to methods in the literature, the method used in this paper follows the lightning surge testing setup in the IEC61000-4-5 standard [8] and concentrates the impact on the converter's internal components.

The rest of this paper is organized as follows. The impact of the lightning surge on the converter is theoretically discussed in Section II. In Section III, the equipment modes used to simulate the lightning test have been introduced. Then, simulations are conducted in Section IV, followed by the conclusion in Section V.

## II. IMPACT ANALYSIS OF THE LIGHTNING SURGE

### A. Converter Configuration

The system configuration is shown in Fig. 1. The three-phase four-wire power conditioning system (PCS) converter is used to connect an 850 V DC grid and the 13.8 kV AC grid. The PCS converter consists of a DC/DC stage and a DC/AC stage, and the DC/DC stage is simplified in this paper since the focus is the DC/AC stage. 10 kV SiC MOSFETs are used at the medium voltage (MV) side, and the nominal MV DC-link voltage is 6.7 kV. The converter power rating is 1 MW, and the AC grid side filter inductance is 4.4 mH (0.009 p.u.), which is mainly determined by the AC grid-side current harmonic requirements.

Based on the system configuration, SIEMENS 3EK7 120-3AC4 surge arresters are selected to protect the converter from the lightning surge [9]. With the arrester installed, based on the arrester datasheet, the induced overvoltage by a lightning surge can be clamped at around 37 kV (at 10 kA).

However, this overvoltage is much higher than the converter normal operation voltage (11.3 kV peak), and it will impact the operation of the PCS converter.

Therefore, it is necessary to evaluate the impact of a lightning surge on the PCS converter, and the converter design needs to consider the impact from lightning so that the converter can protect itself from or even ride through the lightning surge.

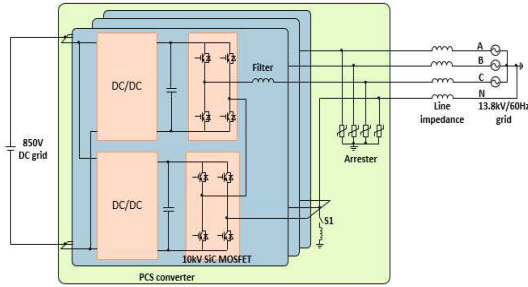


Fig. 1. PCS converter configuration.

### B. Impact on the Phase Current

A large overvoltage at the phase terminal can induce an inrush current due to the large voltage drop on the filter inductor.

Figure 2 shows the simplified power loop of the converter, through which a lightning surge can pass. To simplify the analysis, the DC/DC stages of the PCS converter are represented by current sources and decoupled from the DC/AC stages. Because of the three-phase four-wire configuration, the neutral wire can be grounded through the converter or the AC grid grounding, and an inductor  $L_{ng}$  (could also be resistor or both) represents the neutral line to ground impedance.

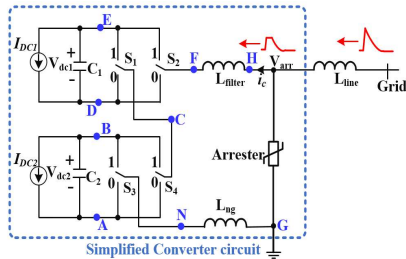


Fig. 2. Simplified surge loop.

When a lightning surge occurs, the arrester absorbs large surge current and clamps the converter terminal voltage  $V_{arr}$  at a certain level, which is dependent on the surge current, for example, 37 kV (at 10 kA). However, 37 kV is still much higher than grid normal operating voltage. And the maximum output voltage of the PCS converter,  $V_{FN}$ , is the sum of the two DC-link voltages, which is 13.4 kV. Then, the filter inductor  $L_{filter}$  and the neutral-to-ground impedance  $L_{ng}$  share the remaining voltage and the phase current  $i_c$  will increase. The inductor current increment during the lightning surge can be estimated as

$$\Delta i_L = \frac{di_c}{dt} \Delta t = \frac{V_{arr} - V_{FN}}{L_{filter} + L_{ng}} = \frac{V_{arr} - (S_2 - S_1)V_{dc1} - (S_4 - S_3)V_{dc2}}{L_{filter} + L_{ng}} \Delta t \quad (1)$$

where  $S_k$  ( $k=1, 2, 3, 4$ ) represent the states of the devices in each half bridge, and

$$S_k = \begin{cases} 1 & \text{If current flow through the upper device} \\ 0 & \text{If current flow through the lower device} \end{cases} \quad (2)$$

Although the lightning surge is quite short in time, the high overvoltage can still induce a large inrush current because of the large voltage and small impedance. From (1), it can be found that the worst case happens when:

1) the neutral-to-ground impedance  $L_{ng}=0$ , which means the PCS converter is solid ground at the neutral point.

2) the converter output voltage,  $V_{FN}$ , has an opposite polarity to the lightning surge voltage.

Since the typical lightning surge has a time characteristic of 1.2/50  $\mu s$ , assuming the arrester clamps the lightning surge at 37 kV for 50  $\mu s$  helps to simplify the calculation of the inrush current. Then, under a positive lightning surge, the current increment during the surge transient in the worst case could be

$$\Delta i_{L1} = \frac{37kV + 6.7kV + 6.7kV}{4.4mH + 0} \times 50 \mu s = 573 A = 9.8 p.u. \quad (3)$$

However, with such a high inrush current, all PWMs can be shut down by the overcurrent protection. Then, the inrush current will flow through the body diodes of the MOSFETs, and this will change the PCS converter output voltage,  $V_{FN}$ , to be the same polarity as the lightning surge voltage. This could help to reduce the rising speed of the current. Assuming the PCS converter output voltage has an opposite polarity to the lightning surge, then the inrush current would be

$$\Delta i_{L2} = \frac{37kV - 6.7kV - 6.7kV}{4.4mH + 0} \times 50 \mu s = 268 A = 4.5 p.u. \quad (4)$$

Then, with solid ground, the PCS converter may have an inrush current within a range of [4.5 p.u., 9.8 p.u.] depending on the switching states of the PCS converter at the moment when the lightning surge happens. Besides, the calculation ignored the saturation characteristic of the filter inductor and assumed the filter inductance is constant even with a high current. However, if the inductor is not designed to have that high saturation current, the inductor may be saturated during the lightning transient and the inrush current will go higher than the calculation.

The inrush current will flow through the filter inductor, devices, busbar, etc. Also, the regular protection components, such as fuse and mechanical switches, do not have the capability to protect the converter from this inrush current because their response time is much larger than the period of a lightning surge. Therefore, if the inrush current induced by the lightning is not considered in the converter design, it could trip or even damage the PCS converter.

From the analysis, it can also be found that the AC grid side filter inductance and the neutral-to-ground impedance are the main impedance to limit the inrush current from a lightning surge. The higher the overall impedance, the smaller the inrush current. Therefore, a larger filter inductance or a higher grounding impedance can help reduce the inrush current caused by a lightning surge.

### C. Impact on the DC-link Voltage

As analyzed above, the inrush current will also flow through the DC-link capacitor, either through the MOSFET channels or through the body diodes. If the devices are switching and the inrush current flows through the device channels, it could either charge or discharge the DC-link voltage depending on the states of the switches. If the PCS converter has stopped switching as a result of overcurrent protection and the inrush current flows through the body diodes of MOSFETs, the inrush current will only charge the DC-link capacitors. In both cases, DC-link overvoltage may happen.

From Fig. 2, the differential equations for the DC-link capacitors are

$$\begin{cases} C_1 \frac{dV_{dc1}}{dt} = (S_2 - S_1)i_c - I_{DC1} \\ C_2 \frac{dV_{dc2}}{dt} = (S_4 - S_3)i_c - I_{DC2} \end{cases} \quad (5)$$

Through solving equations (1) and (5), the overvoltage and overcurrent of the converter can be obtained. However, it is difficult to do that, and simulation could be a good method to do the estimation.

Since the lightning transient is short in time, increasing the DC-link capacitance can significantly reduce the voltage overshoot. Also, increasing the filter inductance can help to reduce the DC-link overvoltage because of the smaller inrush current.

### D. Impact on Converter Insulation Design

Insulation is another important consideration for the medium voltage PCS converter when facing a lightning surge. As introduced above, during a lightning surge, even with the arrester the induced voltage could be around 37 kV (refer to the ground). Therefore, high potential (refer to the ground) may also occur on the converter components, which may also stress the converter insulation.

Since the arrester is connected between the line and ground, the potential, referenced to the ground, of different components in the converter has to be considered. As shown in Fig. 2, different points in the converter have different potentials during the lightning surge, and they can be expressed as

$$\begin{cases} V_{NG} = \frac{L_{ng}}{L_{ng} + L_{filter}} (V_{arr} - S_{21}V_{dc1} - S_{43}V_{dc2}) \\ V_{AG} = V_{NG} - S_3V_{dc2} \\ V_{BG} = V_{NG} + (1 - S_3)V_{dc2} \\ V_{CG} = V_{NG} + S_{43}V_{dc2} \\ V_{DG} = V_{NG} + S_{43}V_{dc2} - S_1V_{dc1} \\ V_{EG} = V_{NG} + S_{43}V_{dc2} + (1 - S_1)V_{dc1} \\ V_{FG} = V_{NG} + S_{43}V_{dc2} + S_{21}V_{dc1} \\ V_{HG} = V_{arr} \end{cases} \quad (6)$$

From (6), it can be found that the converter neutral point potential,  $V_{NG}$ , makes a great difference for the components' potential during the lightning transient.  $V_{NG}$  is mainly determined by the ratio of the neutral-to-ground impedance,  $L_{ng}$ , to the filter inductor impedance,  $L_{filter}$ . A larger ratio of  $L_{ng}$  to  $L_{filter}$  will result in a higher neutral point potential during the lightning transient, and all the components' potential will be increased correspondingly.

On the contrary, a smaller ratio of  $L_{ng}$  to  $L_{filter}$  will get a smaller neutral point potential and it helps to reduce the converter component potentials during the lightning transient. In this case, the filter inductor withstands most of the clamped voltage, by the arrester.

Therefore, although the neutral-to-ground impedance can help to reduce the inrush current, it also increases the neutral point potential during the lightning transient and then increases the insulation requirements (to the ground) for the components in the converter, such as the DC bus, wires, devices, etc. Besides, the converter or grid grounding impedance is mainly determined by the system's temporary overvoltage design, and it is hard to change for the lightning consideration.

## III. COMPONENT MODELS

As shown in Section II, the impact of the lightning surge on the PCS converter can be qualitatively analyzed, but it is difficult to have a quantitative analysis. Therefore, a simulation model, including the grid, PCS converter, lightning emulator, as well as arrester, is essential to study the impact of a lightning surge on the converter operation more accurately.

### A. Arrester Model

There have been some arrester models published in the literature [10]-[12], and the IEEE arrester model in [10], as shown in Fig. 3, is used in this paper to estimate the arrester performance during the lightning transient. This model is recommended to be used in cases where the current surge's time-to-crest is between 0.5  $\mu$ s and 45  $\mu$ s. Therefore, it is good to use in the lightning analysis, in which the current surge has a time-to-crest of about 8  $\mu$ s. The parameters of the components in the model can be calculated according to the arrester physical dimension [10]:

$$\begin{cases} L_0 = \frac{0.2d}{n} \text{ uH} \\ R_0 = \frac{100d}{n} \text{ } \Omega \\ C = \frac{100n}{d} \text{ pF} \\ L_1 = \frac{15d}{n} \text{ uH} \\ R_1 = \frac{65d}{n} \text{ } \Omega \end{cases} \quad (7)$$

where  $d$  is the estimated height of the arrester in meters, and  $n$  is the number of parallel columns of metal oxide in the arrester. The two non-linear resistors,  $A_0$  and  $A_1$ , can be calculated based on the curve given in [10].

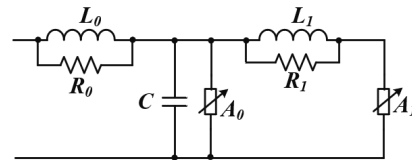


Fig. 3. IEEE arrester model [10].

The parameters for  $R$ ,  $L$ ,  $C$ , and the non-linear resistor  $A_0$  and  $A_1$  of the arrester selected in this paper, SIEMENS 3EK7 120-3AC4, are shown in Table I and Table II, respectively.

TABLE I. PARAMETERS FOR THE R, L, AND C IN THE MODE

Parameter	Value
$L_0$	0.04 $\mu$ H
$R_0$	20 $\Omega$
$C$	500 pF
$L_1$	3 $\mu$ H
$R_1$	13 $\Omega$

TABLE II. PARAMETERS FOR NON-LINEAR RESISTORS IN THE MODE

Current (kA)	$A_0$ Voltage (kV)	$A_1$ voltage (kV)
0.01	32.64	/
0.1	35.90	28.67
1	39.17	31.71
2	40.56	33.34
4	41.96	34.50
6	42.43	34.97
8	43.60	35.67
10	44.29	36.13
12	44.99	36.37
14	45.92	36.83
16	46.63	37.07
18	47.79	37.30
20	48.96	37.53

B. Combined Wave Generator Model

To simulate the lightning surge in the simulation, a lightning surge model needs to be applied. In this paper, the combined wave generator (CWG) model in IEC 61000-4-5 standard is used [8]. As shown in Fig. 4, a DC source will pre-charge a capacitor,  $C$ , through the resistor,  $R_0$ . After the capacitor is fully charged, the switch  $S$  can be closed at some moment to discharge the capacitor through the output terminal and a lightning surge will be generated. Parameters of the  $R$ ,  $C$ , and  $L$  in the model are determined to meet two requirements:

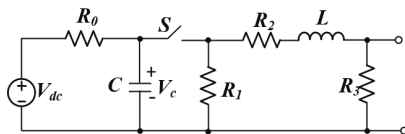


Fig. 4. CWG model [8].

- 1) The CWG outputs a 1.2/50  $\mu$ s voltage surge at open circuit.
- 2) The CWG outputs an 8/20  $\mu$ s current surge at short circuit.

Although the parameter values are not given in the standard, some literature discussed the determination of the parameters [13]-[15]. However, since the IEC 61000-4-5 standard has different versions, and there are some differences between the latest version and the old version, it is important to notice that some literature may design or select parameters to meet the testing requirements in old standards.

This paper uses the parameters calculated in [14], which meets the latest standard, i.e., IEC 61000-4-5 (2014). Based on the system voltage level, a lightning surge peak voltage of 95 kV needs to be generated. The DC source and the pre-charge resistor,  $R_c$ , are eliminated in the simulation model. Instead, an initial voltage  $V_c$  has been given to the capacitor. The CWG parameters are shown in Table III.

TABLE III. PARAMETERS FOR THE CWG

Parameter	Value
$V_c$	101 kV
$C$	9.98 $\mu$ F
$R_1$	9.39 $\Omega$
$R_2$	0.832 $\Omega$
$L$	10.7 $\mu$ H
$R_3$	25.5 $\Omega$

C. Coupling and Decoupling Network

Since the lightning surge testing is conducted when the converter is under operation, a coupling and decoupling network (CDN), as shown in Figure 5, is essential to connect the CWG to the converter testing terminals and reduce the impact to the other equipment in the grid.

The coupling network provides a path for the lightning surge to flow to the converter, and the decoupling network acts as an LC low pass filter to prevent the lightning surge from flowing to the grid side. The determination of the CDN parameters has also been discussed in the literature [16].

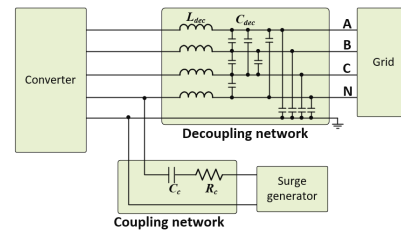


Fig. 5. CDN and its connection.

IV. SIMULATION RESULTS

A. The CWG Model Simulation

With the parameters shown in Table III, the open-circuit and short circuit output of the CWG model has been first simulated on the MATLAB/Simulink, as shown in Fig 6. Based on the requirement of the IEC 61000-4-5 standard, an 18  $\mu$ F capacitor needs to be connected in series with the CWG output terminal in both the open-circuit voltage and short-circuit current test.

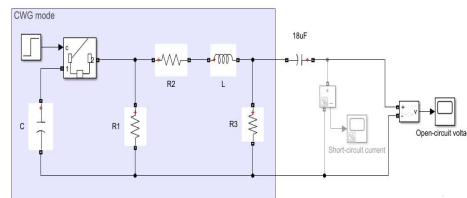


Fig. 6. CWG simulation results.

Fig. 7 (a) and (b) show the waveforms of open-circuit output voltage and short-circuit output current, respectively. Table IV shows the comparison of the performance characteristics between the CWG model and the standard requirement. It can be found that most of the performance can meet the requirement, and only the undershoot of the short-circuit current exceeds the required range. This has been discussed in [16], and it does not impact the analysis in the simulation.

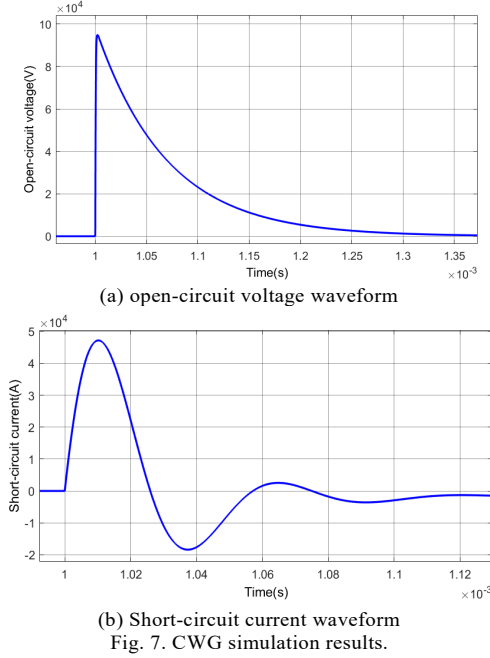


TABLE IV. PERFORMANCE COMPARISON BETWEEN THE CWG MODEL AND STANDARD REQUIREMENT

	Parameter	Standard requirement	CWG model
Open-circuit voltage	Rise time (30% to 90%)	$0.72 \mu\text{s} \pm 30\%$	$0.72 \mu\text{s}$
	Duration (50% to 50%)	$50 \mu\text{s} \pm 20\%$	$50.00 \mu\text{s}$
	Undershoot	$0 \sim 30\%$	0
Short-circuit current	Rise time (10% to 90%)	$6.4 \mu\text{s} \pm 20\%$	$6.32 \mu\text{s}$
	Duration (50% to 50%)	$16.9 \mu\text{s} \pm 20\%$	$16.70 \mu\text{s}$
	Undershoot	$0 \sim 30\%$	39%

### B. Arrester Model Simulation

To check the accuracy of the arrester mode, a separate simulation has been conducted. As shown in Fig. 8, an  $8/20 \mu\text{s}$  current surge generator, based on the mathematic curve and a controllable current source, is used to generate different peak inrush currents to test the arrester. The arrester terminal voltage waveform under an  $8/20 \mu\text{s}$  lightning surge current with a peak of 10 kA is shown in Fig. 9. The arrester clamps the terminal voltage at around 39 kV. Other inrush currents with different peak values have also been tested, and the arrester peak voltages are recorded. As shown in Table V, the arrester model peak voltages are close to the value given in the arrester datasheet, and the maximum deviation is less than 5%.

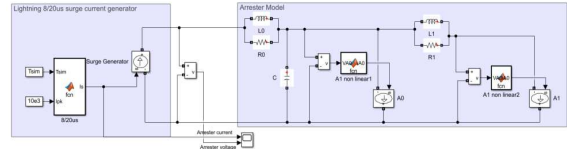


Fig. 8. Arrester model simulation.

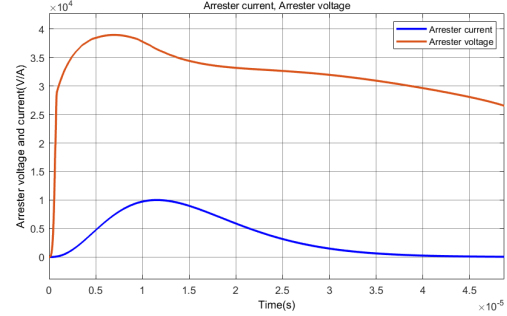


Fig. 9. Arrester model terminal voltage @  $8/20 \mu\text{s}$ , 10 kA.

TABLE V. PERFORMANCE COMPARISON BETWEEN THE CWG MODEL AND STANDARD REQUIREMENT

Lightning Surge	Arrester Datasheet	Arrester model	Deviation
$8/20 \mu\text{s}$ @ 1.5 kA	31.7 kV	32.8 kV	+3.5%
$8/20 \mu\text{s}$ @ 3 kA	33.2 kV	34.4 kV	+3.6%
$8/20 \mu\text{s}$ @ 5 kA	34.7 kV	36.1 kV	+4.0%
$8/20 \mu\text{s}$ @ 10 kA	37.3 kV	39.0 kV	+4.6%
$8/20 \mu\text{s}$ @ 20 kA	42.9 kV	42.2 kV	-1.6%

### C. PCS Converter Simulation Model

The PCS converter DC/AC stage, arrester, CWG, CDN, and the grid are assembled in the simulation to simulate the lightning impact on the converter operation. Fig. 10 shows the system configuration, and the lightning surge has been applied between the line and ground.

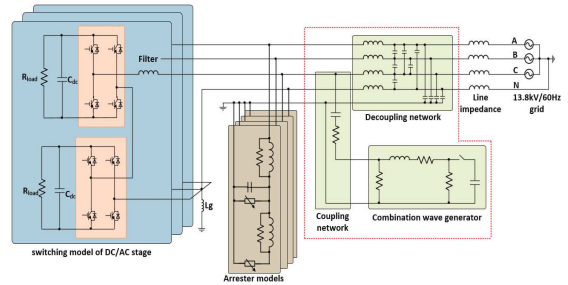


Fig. 10. Lightning surge simulation diagram.

With the neutral point solid grounded, the PCS converter has been tested with and without the arrester. Fig. 11 shows the voltage clamping of the arrester. Without the arrester, during the lightning surge, the converter terminal voltage will have a peak value of around 95 kV. However, with the arrester, the inrush voltage is clamped at around 37 kV, and the surge current flowing through the arrester is around 5.5 kA.

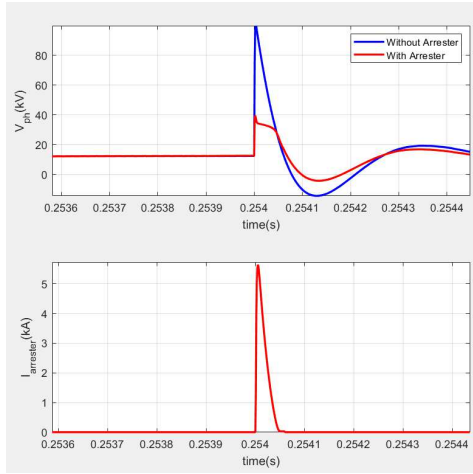


Fig. 11. Phase voltage and arrester current.

#### D. Inrush Current and DC-link Overvoltage

Fig. 12 shows the waveforms of phase voltages, phase currents, and DC-link voltages. An inrush current up to 6 p.u. is induced during the lightning transient, and the DC-link voltages of phase C (lightning surge phase) has a voltage overshoot of around 500 V. This verifies the inrush current and DC-link voltage overshoot analysis in Section II.

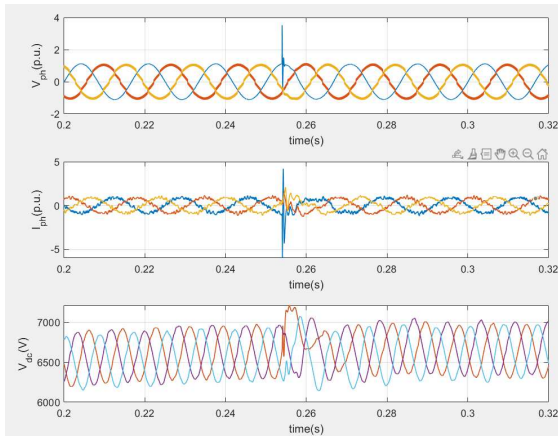


Fig. 12. Phase voltages, currents, and DC-link voltages.

#### E. Converter Insulation

To evaluate the impact of a lightning surge on the PCS converter insulation. Instead of solid grounding, different neutral-to-ground impedances are used in the simulation. Fig. 13 and Fig. 14 show the waveforms of AC voltages, AC currents, and the neutral point potential of the PCS converter under different neutral-to-ground impedances.

In Fig. 13, the neutral-to-ground impedance is 0.5 mH, and during the lightning surge, the neutral point potential is around 0.2 p.u. The inrush current is around 4.7 p.u., which is smaller than the value, 6 p.u. in Fig. 12, in the case where the neutral point is solidly grounded. With a larger neutral-to-ground impedance, as shown in Fig. 14, the neutral point potential increases to around 0.55 p.u. while the inrush current reduced to 4.0 p.u.

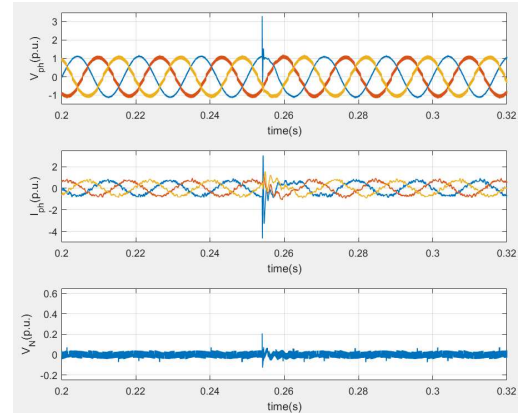


Fig. 13. 0.5 mH neutral-to-ground impedance.

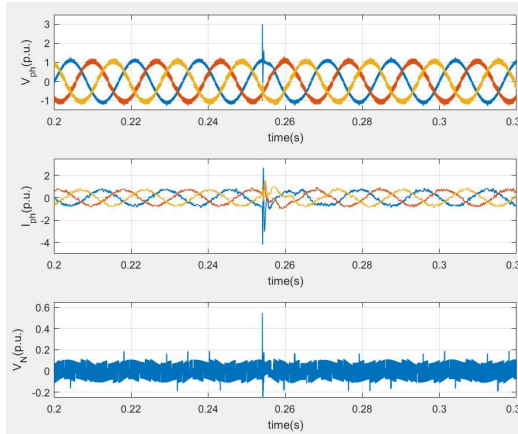


Fig. 14. 1.5 mH neutral-to-ground impedance.

Therefore, as shown in Table VI, the larger the neutral-to-ground impedance, the smaller the inrush current but the higher neutral point potential, which increases the potential of other components in the converter. This verifies the theoretical analysis in Section II.

TABLE VI. INSULATION SIMULATION SUMMARY

Neutral-to-ground impedance	Inrush current	Neutral point potential
0	6 p.u.	0
0.5 mH	4.7 p.u.	0.2 p.u.
1.5 mH	4.0 p.u.	0.55 p.u.

#### V. CONCLUSION

In this paper, the impact of the lightning surge on a 10 kV SiC MOSFET-based 13.8 kV three-phase four-wire grid-connected converter is analyzed. It is concluded that the clamped voltage by the arrester is still much higher than the converter normal operating voltage. When the control neutral point is solidly grounded, a large inrush current, up to 6 p.u., could be induced by the clamped voltage. The inrush current flows through the converter and the DC-link voltage overshoot could also occur. Also, the neutral-to-ground impedance impacts both the inrush current and the internal component's potential to the ground. The higher the neutral-to-ground impedance, the smaller the inrush current while the larger the neutral point potential, which requires higher insulation for the components in the converter. The approach

used in this paper can also be used to analyze the lightning impact for other grid-connected converters.

#### ACKNOWLEDGMENT

This work was supported primarily by the Advanced Manufacturing Office (AMO), United States Department of Energy, under Award no. DE-EE0008410. This work made use of the shared facilities of the Engineering Research Centre Program of the National Science Foundation and the Department of Energy under NSF Award no. EEC-1041877. The authors would like to acknowledge the contribution of Southern Company and Powerex.

#### REFERENCES

- [1] J. Thoma, B. Volzer, D. Kranzer, D. Derix, and A. Hensel, "Design and Commissioning of a 10 kV Three-Phase Transformerless Inverter with 15 kV Silicon Carbide MOSFETs," in 20th European Conference on Power Electronics and Applications (EPE'18 ECCE Europe), 2018, pp. P.1-P.7.
- [2] M. Davari, O. A. Mousavi, and I. Salabeigi, "Analysis and comparison of the lightning overvoltage in the AC connected and VSC based HVDC connected wind farms," in TENCON IEEE Region 10 Conference, 2009, pp. 1-6.
- [3] J. Birkl, E. Shulzhenko, J. Kolb, and M. Rock, "Approach for evaluation of lightning current distribution on wind turbine with numerical model," in 33rd International Conference on Lightning Protection (ICLP), 2016, pp. 1-8.
- [4] M. S. M. Nasir, M. Z. A. Ab-Kadir, M. A. M. Radzi, M. Izadi, N. I. Ahmad, and N. H. Zaini, "Lightning performance analysis of a rooftop grid-connected solar photovoltaic without external lightning protection system," PLOS ONE, vol. 14, no. 7, p. e0219326, 2019.
- [5] H. Zaini et al., "Lightning Surge Analysis on a Large Scale Grid-Connected Solar Photovoltaic System," Energies, vol. 10, p. 2149, 12/15 2017.
- [6] S. Fei and Z. Hao, "Simulation on lightning overvoltage of  $\pm 800$ kV converter station," in 7th Asia-Pacific International Conference on Lightning, 2011, pp. 491-495.
- [7] X. Chen, C. Xia, W. Shi, T. Lu, T. Lei, and X. Zhao, "Study on Direct Lightning Protection of  $\pm 1100$ kV Converter Station Grid," in 11th Asia-Pacific International Conference on Lightning (APL), 2019, pp. 1-5.
- [8] Electromagnetic compatibility (EMC)-Part 4-5: Testing and measurement techniques – Surge immunity test, IEC 61000-4-5, 2014.
- [9] Metal-Oxide Surge Arresters in High-Voltage Power Systems, 3rd ed., SIEMENS, Erlangen, Germany, 2012.
- [10] "Modeling of metal oxide surge arresters," IEEE Transactions on Power Delivery, vol. 7, no. 1, pp. 302-309, 1992.
- [11] P. Pinceti and M. Giannettoni, "A simplified model for zinc oxide surge arresters," in IEEE Transactions on Power Delivery, vol. 14, no. 2, pp. 393-398, April 1999.
- [12] P. Unahalekhaka, "Simplified Modeling of Metal Oxide Surge Arresters," Energy Procedia, vol. 56, pp. 92-101, 2014.
- [13] X. Pan, T. Rinkleff, B. Willmann and R. Vick, "PSpice simulation of surge testing for electrical vehicles," International Symposium on Electromagnetic Compatibility - EMC EUROPE, Rome, Italy, 2012, pp. 1-6.
- [14] N. Marukatat, P. Tuethong and P. Yutthagowith, "Design and Construction of a Combination Wave Generator," International Universities Power Engineering Conference (UPEC), Bucharest, Romania, 2019, pp. 1-5.
- [15] C. F. M. Carobbi and A. Bonci, "Elementary and ideal equivalent circuit model of the 1, 2/50-8/20  $\mu$ s combination wave generator," in IEEE Electromagnetic Compatibility Magazine, vol. 2, no. 4, pp. 51-57, 2013.
- [16] Mi Zhou, Jianguo Wang, Yang Liu and Fang Liu, "Coupling and decoupling network for surge immunity test on power lines," International Conference on Electrical Machines and Systems, Wuhan, China, 2008, pp. 151-155.